Materials LAB

REVIEW ARTICLE

Materials Lab 2023, 2, 220055

Cathode choices for rechargeable aluminium batteries: the past decade and future

Yueqi Kong, Nashaat Ahmed Gadelhak, Shuimei Chen, Dmitrii Rakov, Ashok Kumar Nanjundan*, Chengzhong Yu and Xiaodan Huang*

Rechargeable aluminium batteries are a promising alternative battery technology compared to lithium-ion batteries, because of the high theoretical capacity, low cost and high safety of aluminium. The past decade has witnessed the rapid development of rechargeable aluminium battery technology with the focus on exploring high performance cathode materials and investigating their charge storage mechanisms. However, the challenges in the cathode research including inadequate capacity, sluggish reaction kinetics and inferior cycling stability still remain. Various strategies have been attempted to address these challenges to realize the advantages of rechargeable aluminium batteries. The present review aims to collect the comprehensive body of research performed in the literature hitherto to develop interaction/conversion/coordination type cathodes for rechargeable aluminium batteries. Future research directions and prospects in rechargeable aluminium battery field are also proposed.

A special report released by Intergovernmental Panel on Climate Change (IPCC) in 2018 calls for building a net-zero emissions society by 2050 if the world is to limit global warming to 1.5 °C above pre-industrial levels.[1] The priority action to ensure the opportunity of net-zero emissions is to expand the exploration and utilization of renewables like solar and wind instead of fossil fuels.[2] Since renewable energy resources are intermittent in nature, they are not constantly predictable and available. Consequently, advanced energy storage systems (ESSs) are generally required to assist with the integration of these renewable sources into power systems. The rechargeable battery is one of the most investigated and relatively mature ESSs. Currently, rechargeable batteries in the markets are dominated by lithium-ion batteries (LIBs), which serve from portable electronic products to electric and hybrid vehicles. However, LIBs still suffer from high cost, scarce lithium (Li) resources and safety concerns, restricting their further development.[3–6] All these drawbacks of LIBs have spurred an increase in research focus on utilizing more earth-abundant metals to develop alternative battery technologies with cost-effectiveness, safety, high energy density and environmental friendliness.[7–11]

Competitive metal candidates include aluminium (Al), sodium (Na), magnesium (Mg), potassium (K), calcium (Ca) and zinc (Zn). Among these non-lithium metals, Al has distinctive advantages. Fig. 1 summarizes the detailed comparison between Al and other active metals in terms of their gravimetric and volumetric capacity, abundance and cost.[12–15] Al has a high gravimetric capacity (2980 mAh g^{-1}, only slightly lower than 3862 mAh g^{-1} of Li) and the highest volumetric capacity (8040 mAh cm^{-3}, ~4 times of 2042 mAh cm^{-3} of Li), benefiting from its light atomic mass and three-electron redox property.[16] More importantly, Al is the most abundant metal element in the earth crust (82 000 ppm, >1200 times higher than Li), which makes it relatively inexpensive for production. Additionally, Al metal can be directly used as the anode in non-volatile and non-flammable ionic liquid chloroaluminate electrolytes, offering significant safety improvements over LIBs. Hence, rechargeable aluminium batteries (RABs) hold promising potential as low cost, high safety and high energy density ESS to replace LIBs.

The development history of RAB technology is briefly summarized in Fig. 2. The studies of RABs could date back to 1857 when Al was initially used as anode in the Buff cell (Al-HNO_3-C).[17] In 1948, Heise et al. developed the heavy-duty Al-Cl_2 battery with amalgamated Al as the anode, demonstrating a high open-circuit voltage of 2.45 V.[18] Efforts were then made on utilizing Al anodes in primary batteries after 1951 when a Leclanche-type dry cell (Al-aqueous NaOH-MnO_2 (C)) was disclosed.[19] Inspired by previous work, Zaromb invented the first Al-air cell in concentrated alkali solution in the 1960s.[20] However, all these early attempts did not succeed to be utilized in any practical batteries, which is mainly due to the formation of a dense passivating layer (Al_2O_3) in aqueous electrolytes. The poorly ion-conducting oxide film is not be-

Australian Institute for Bioengineering and Nanotechnology, The University of Queensland, Brisbane, QLD 4072, Australia

* Corresponding author, E-mail: ashok.nanjundan@uq.edu.au; x.huang@uq.edu.au

Received 13 September 2022; Accepted 8 December 2022; Published online

DOI: 10.54227/mlab.20220055

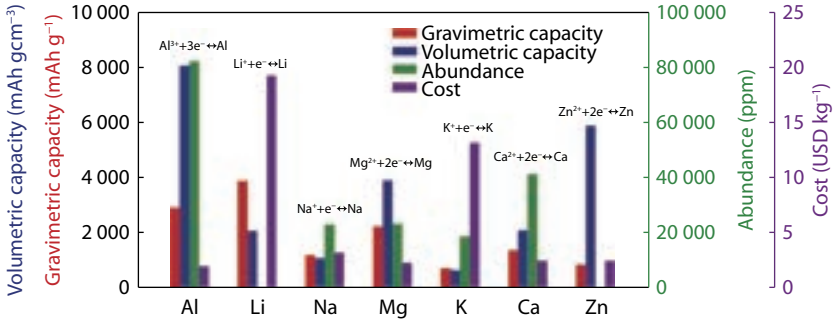

Fig. 1 Comparison of Al and other metal anodes in electrochemical systems in terms of gravimetric and volumetric capacity, abundance, and cost.

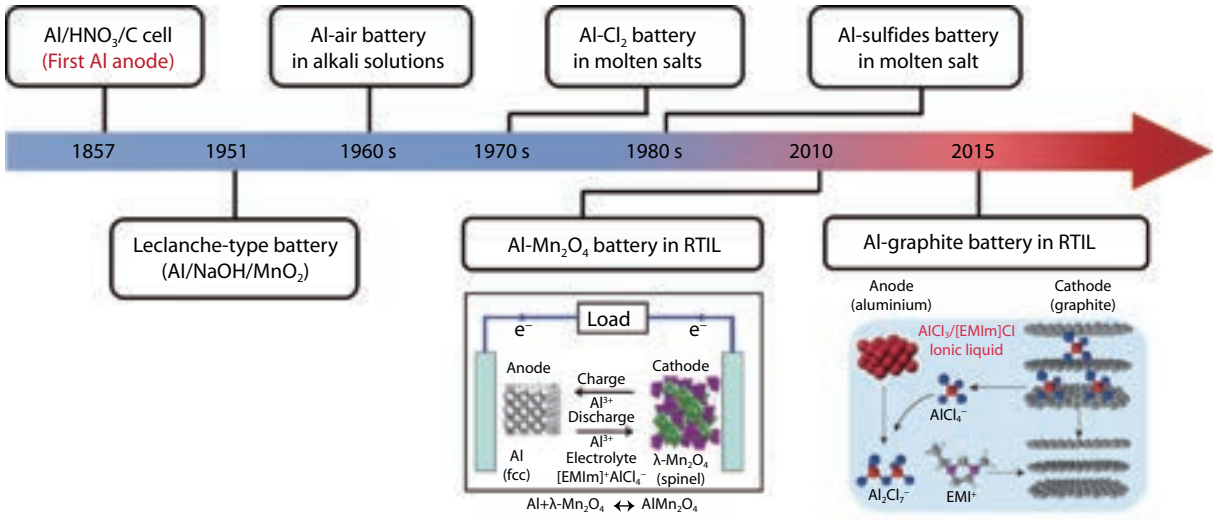

Fig. 2 A brief history of Aluminum battery developments.[16,27] Copyright 2015, Nature Publishing Group. Copyright 2010, IOP Publishing.

neficial for Al^{3+} migration, leading to the failure of the Al anode to be recharged.

In the 1970s, the usage of high-temperature molten salts as non-aqueous electrolytes was demonstrated, which avoided the formation of passivating Al_2O_3 layer on the Al surface, and more importantly, guaranteed the reversible Al plating/stripping behaviors because of the fast ion transportation boosted by high operation temperature.[21,22] On the premise of these early attempts to provide fundamental bases, the prototype of RABs (Al-$AlCl_3$/NaCl-FeS_2) was constructed by Kuora in 1980, exhibiting a high discharge plateau of ~1.1 V above 270 °C.[23] To lower the working temperature, Kuora and Takami then adopted $AlCl_3$/MCl/1-butylpyridinium (BPC) (M = Li and Na) ternary melts as the electrolyte for an Al-FeS_2 rechargeable cell, operating around 100 °C.[24] It has been demonstrated that both the operating temperature and BPC concentration matter for the charge-discharge characteristics. However, the $AlCl_3$/alkali metal halide system still causes issues of increasing energy consumption and complexing battery operation, and hence the research focus was later turned to searching for suitable non-aqueous electrolytes that could be used at room temperature.

In 1984, Qin's group and Dymek's group reported that mixing $AlCl_3$ with organic salts (n-butylpyridinium chloride ([BPy]Cl) or 1-methyl-3-ethylimidazolium chloride ([EMIm]Cl)) could form chloroaluminate ionic liquid at room temperature, which can serve as the electrolyte for Al plating/stripping (named as room temperature ionic liquid (RTIL) electrolyte).[25,26] Despite the settlement of reversible anode reaction, there is almost no significant progress in RABs in the following two decades, because of the lack of appropriate cathode materials. In 2010, the secondary RAB concept was proposed in a meeting abstract by Paranthanman et al. They constructed an Al-MnO_2 cell in RTIL of $AlCl_3$/[EMIm]Cl with a molar ratio of 2:1.[27] Unfortunately, their initial test shows no intercalation capacity from the MnO_2 cathode. Until 2015, Dai's group reported the Al-$AlCl_3$/[EMIm]Cl-graphite cell as rechargeable AIBs, exhibiting outstanding electrochemical properties of high voltage (~2.0 V) and high rate/cycling performance (~60 mAh g^{-1} of capacity at 4 A g^{-1} for 7500 cycles).[16] Since then, extensive efforts have been paid to cathodes, anodes and RTIL electrolytes of non-aqueous RABs to improve the electrochemical performance. Aluminium-based batteries in aqueous media, including Al-air batteries and aqueous Al-ion batteries, have also attracted attention in recent years. However, its overall performance was hindered by two major problems using Al as an anode. First is the formation of a passivating oxide layer in an aqueous environment, reducing the operating voltage and increasing both charge and mass transfer resistance. The second issue is the hydro-

DOI: 10.54227/mlab.20220055

gen evolution that occurs during the battery operation. In this review, we mainly focus on RAB with nonaqueous ionic liquid electrolytes. In the following content of this article, the "RAB" represents the non-aqueous RAB based on RTIL electrolytes unless otherwise stated.

The typical configuration of a RAB is composed of an Al metal anode, chloroaluminate electrolyte and a suitable cathode, as shown in Fig. 3. Among these battery components, cathodes play a crucial role in determining the battery capacity and have consequently become the major focus in RAB research.[28] A broad range of cathode materials including graphitic carbons, chalcogens, metal chalcogenides and organic compounds, and their charge storage mechanism in RABs, have been extensively investigated. According to the working mechanism, the reported RAB cathode materials can be generally classified into three major types: the intercalation-type, the conversion-type and the coordination-type cathodes. The specific redox mechanisms, advantages and challenges are presented in Fig. 4 for a comprehensive comparison. Despite of many recent progresses in this research area, there are still challenges that stand in the way of the development of each type of RAB cathode materials. Previous review articles of cathode materials in RABs usually elaborate based on the chemical or structural composition, or mainly focus on a certain type of cathode materials. In view of it, a comprehensive review to summarize the current research state of all three types of RAB cathodes is necessary. This review aims to compose a panoramic view of the development of cathode materials for RABs, elaborating the investigation of charge storage mechanism, the strategies to improve electrochemical performances, and proposing the future perspectives toward advanced RAB technology.

Intercalation-type cathode

Intercalation-type cathodes (ITCs) are primarily relying on a charge storage mechanism of ion intercalation/de-intercalation. During the charging/discharging processes, mobile guests are reversibly intercalated/de-intercalated into/out of the lattice or channels of ITCs. ITCs in RABs can be classified into two categories based on the mobile guest, namely $AlCl_4^-$-based ITC and Al^{3+}-based ITC.

$AlCl_4^-$-based intercalation-type cathode

Graphitic carbon (GC) materials have been paid numerous attention as intercalation-type electrodes in rechargeable batteries on account of their high conductivity, layered structure, and mature preparation technology. In 2015, Dai's group adopted a 3D graphitic foam (Fig. 5a) as the cathode, an Al foil as the anode, and RTIL ($AlCl_3$/[EMIm]Cl) as the electrolyte to assemble RABs.[16] They first proposed that the mechanism of the GC cathode is the reversible intercalation/de-intercalation of $AlCl_4^-$ ions within the layered graphitic lattice (Fig. 5b). The redox reactions of the Al-graphite cell during battery operation can be written as:

$$\text{Anode}: \ 4Al_2Cl_7^- + 3e^- \leftrightarrow Al + 7AlCl_4^-$$

$$\text{Cathode}: \ C_n + AlCl_4^- \leftrightarrow C_n[AlCl_4] + e^-$$

Such a RAB cell demonstrates a high discharge voltage plateau (>2.0 V), ultra-fast charge-discharge property (<1 min) and outstanding cycling stability (~100% capacity retention

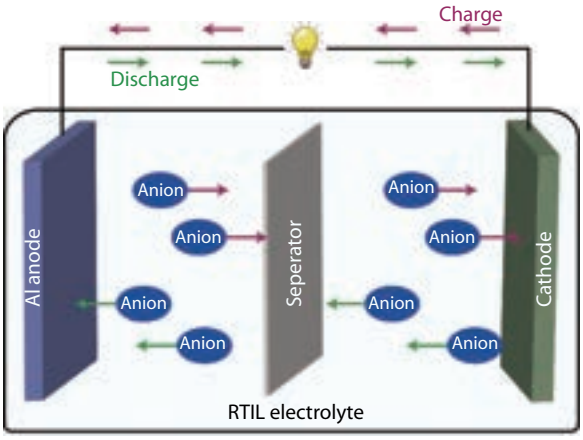

Fig. 3 Typical configuration of a RAB cell using chloroaluminate anions as the charge carrier.

over 7500 cycles). Since then, this breakthrough has made RABs gain worldwide attention. Despite exceptional achievements in Dai and co-workers' study, the CVD technology they used to produce GC is low-yield and energy-consuming. Subsequently, they reported a more economic monolithic 3D graphitic foam prepared through anion pre-intercalation into graphite followed by thermal expansion and hydrogen evolution reaction. With the highly porous structures that could facilitate ion diffusion and insertion/extraction kinetics, such a cathode shows higher rate stability at a current density up to 12 A g^{-1} for over 4000 cycles. However, the specific capacities in these pioneering works are quite low (~60 mAh g^{-1}), which still needs to be improved.

A major reason for the limited specific capacity is that GCs failed to provide sufficient active sites for intercalating $AlCl_4^-$ ions. During charging, $AlCl_4^-$ ions can only penetrate from the edge of GC, and the initially intercalated ions will establish the repulsive potential to restrict the penetration of subsequent $AlCl_4^-$ ions. In this regard, micro-/nano-porous structures were designed to introduce more edges into graphene cathodes. Lu's group used nickel (Ni) micro-particles as the template to synthesize an edge-rich graphene paper as the cathode for RABs (Fig. 6a).[29] The interconnected structure and edge-rich feature of graphene lead to high current transportation and increased active sites for $AlCl_4^-$ intercalation/de-intercalation, achieving a capacity of 90 mAh g^{-1} at 8 A g^{-1} for 20000 cycles. They also purposely created in-plane nanovoids throughout the graphene foam by Ar^+-plasma etching (Fig. 6b).[30] The nanovoids could serve as expressways and active sites for $AlCl_4^-$ intercalation, and thus achieving a high specific capacity of 148 mAh g^{-1} at 2 A g^{-1}. However, the 3D graphene foam used in this work possesses large macropores (several microns) because of using the metal foam as templates, resulting in low density and low volumetric capacity (~0.74 mAh cm^{-3}). Huang et al. prepared a monolithic nanoporous graphene foam by hydrothermal treatment of graphene oxide and silica followed by high-temperature annealing and silica etching.[31] The obtained 3D graphene foam has a smaller pore size of 94 nm and an improved density of 81 mg cm^{-3} than CVD-grown ones[32]. When applied this monolithic graphene foam as the AIB cathode, a volumetric capacity of up to 12.2 mAh cm^{-3} and a gravimetric capacity of 151 mAh g^{-1}

DOI: 10.54227/mlab.20220055

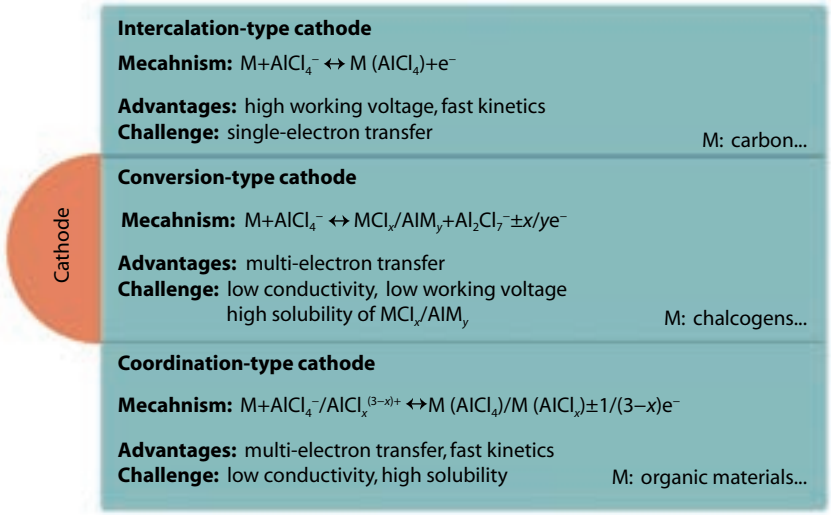

Fig. 4 The comparison of the redox mechanisms, advantages and challenges of different types of cathodes in RABs.

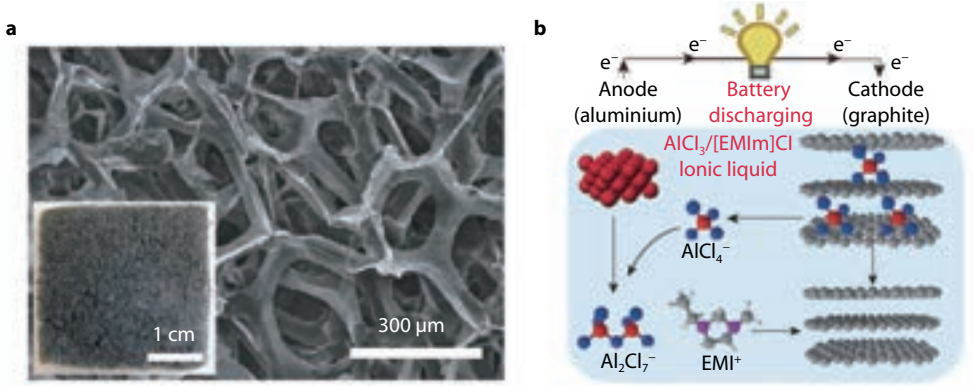

Fig. 5 **a** SEM image of 3D graphitic foam; scale bar, 300 μm. Inset, photograph of 3D graphitic foam; scale bar, 1 cm. **b** Working mechanism of Al-graphite cell.[16] Copyright 2015, Nature Publishing Group.

were achieved.

In addition to the modulation of porous structures, regulating the size of graphene sheet in the vertical (c-axis) dimension was proved to be another effective way to improve the $AlCl_4^-$ storage capability. Liu's group compared the electrochemical performances of few-layer graphene and thick graphite in RABs, and unveiled that decreasing the size of c-axis could facilitate the kinetics of anion intercalation/de-intercalation, thus improving the $AlCl_4^-$ storage capability (Fig. 6c).[33] Afterwards, Rao et al. reported a few-layer graphene foam cathode, delivering a specific capacity of 106 mAh g^{-1} at the current density of 0.2 A g^{-1}.[34] Furthermore, several groups have demonstrated that the quality of graphene also matters for high $AlCl_4^-$ storage capability.[35–40] Gao's group proposed that functional groups and dopant impurities in graphene are detrimental for $AlCl_4^-$ storage, and designed a defect-free graphene cathode for RABs (Fig. 6d).[35] They processed the graphene oxide at an ultra-high temperature of 3000 °C (GA3000) to remove inactive defects and obtain completely crystallized sp^2 carbons. The GA3000 cathode delivers a higher specific capacity (100 mAh g^{-1}) than its defective counterparts (45 and 80 mAh g^{-1}) at the current density of 5 A g^{-1}. Gao et al. further designed a "trihigh tricontinueous" (3H3C) graphene film, featuring high quality, orientation and channeling for local structures (3H) and continuous electron-conduction electron-conducting matrix, ion-diffusion highway and electroactive mass (3C) (Fig. 6e).[36] Such a cathode shows a superior specific capacity of 120 mAh g^{-1} over GA3000. Rao's group showed straightforward evidence of detrimental effects of nitrogen (N) dopants in graphene on $AlCl_4^-$ insertion/extraction processes.[34] N-doped graphene cathodes show inferior charge/discharge characteristics than undoped ones, which is attributed to the reduced anion mobility and catalytically decomposition of $AlCl_4^-$ anions to produce Cl_2 in the presence of N doping. Functional groups, particularly oxygen-containing groups in graphene, were also proved to show negative effects on the electrochemical performance of RABs. A graphene aerogel cathode with an oxygen atomic ratio of 12.5 % was synthesized by Wu et al.[38] Although this cathode delivers a high capacity of 145 mAh g^{-1} at 1 A g^{-1}, it has no obvious charge/discharge plateaus, suggesting a capacitive behaviour rather than a battery behaviour. Wu et al. have taken both the few layer and high quality features of graphene cathode into consideration and prepared a high quality few-layer graphene through electrochemical exfoliation of graphite.[41] The resulting graphene

DOI: 10.54227/mlab.20220055

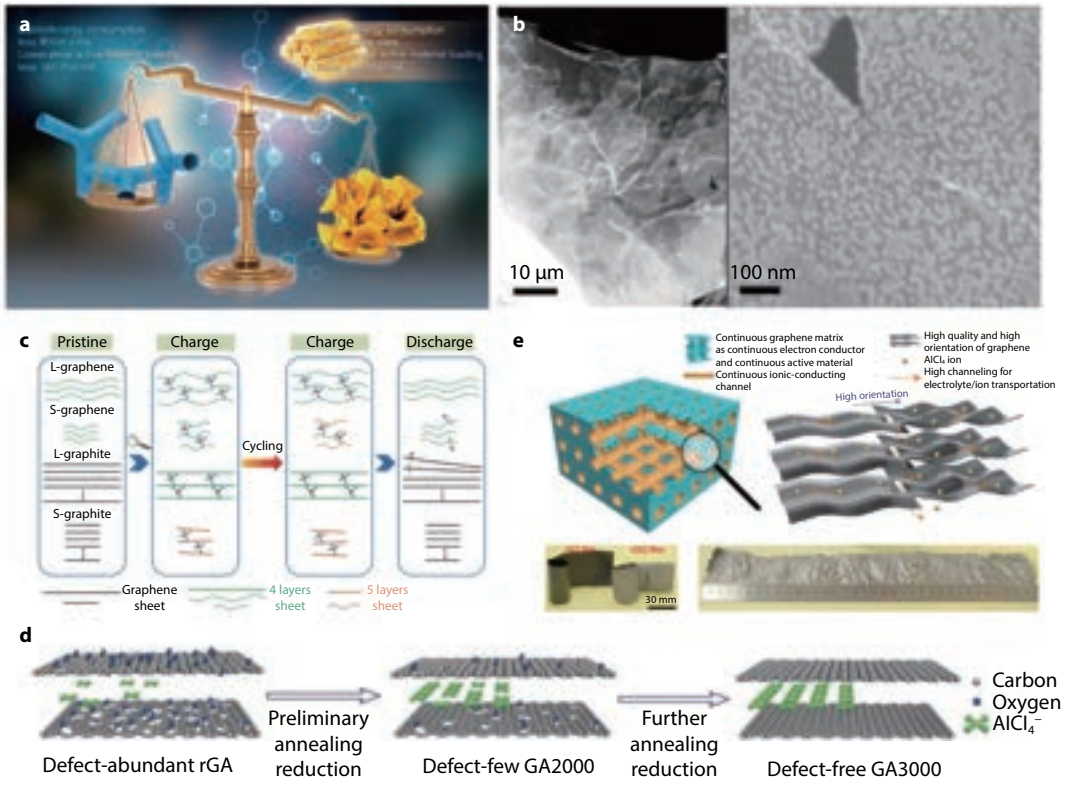

Fig. 6 **a** Scheme of edge-rich graphene and CVD-grown graphene foam for RABs.[29] Copyright 2018, Elsevier. **b** SEM images showing in-plane nanovoids formation throughout the graphene foam after Ar^+-plasma etching.[30] Copyright 2017, Wiley-VCH Verlag GmbH & Co. **c** Schematics of $AlCl_4^-$ intercalation chemistry in few-layer graphene and thick graphite cathode.[33] Copyright 2017, Wiley-VCH Verlag GmbH & Co. **d** Schematic of defect-free graphene design.[35] Copyright 2017, Wiley-VCH Verlag GmbH & Co. **e** "3H3C" design and photograph of graphene cathode.[36] Copyright 2017, American Association for the Advancement of Science.

nanosheets exhibit 3-5 layers, high crystallinity (ID/IG from Raman spectroscopy < 0.05), and an extremely low O atom ratio (~2%). When applied as the cathode for RABs, a high specific capacity of 173 mAh g^{-1} at 1 A g^{-1} was obtained.

Apart from GCs, some metal compounds, such as SnS_2[42], SnS[43], $Cu_{2-x}Se$[44], WO_{3-x}[45], $CoSe_2$[46], Cu_3P[47], WS_2[48], NiTe[49], SnSe[50], etc, have been demonstrated as RAB cathodes working as $AlCl_4^-$ intercalation mechanism. The electrochemical performances of these cathodes as well as reported GC cathodes are summarized in Table 1. Compared with GCs, metal chalcogenides achieve higher initial specific capacities (200~500 mAh g^{-1}) due to their larger interlayer space or structural channels. However, none of them is satisfactory for RABs due to their inferior conductivity, structural instability, and low discharge voltage plateaus (<1.0 V), leading to low-rate performance (capacities decrease drastically from low to high current density) and poor cycling stability. In summary, GCs are the most reported cathodes for AIBs based on $AlCl_4^-$ intercalation and have demonstrated appealing electrochemical performances of high voltage, fast charge/discharge rate and long cycling stability. Nonetheless, state-of-the-art GC cathodes can only reach limited specific capacities of 60 to 170 mAh g^{-1}, which are far insufficient for powering RABs with comparable energy density to LIBs.

Al^{3+}-based intercalation-type cathode

Compared with monovalent $AlCl_4^-$, the intercalation of trivalent Al^{3+} readily possesses more efficient aluminium storage, resulting in a higher specific capacity. The ionic radius of Al^{3+} (0.53 Å) is much smaller than that of $AlCl_4^-$ (5.28 Å), but the strong electrostatic interactions between high formal-charge Al^{3+} and the ionic substructures of the host material often limit the Al^{3+} intercalation. Nevertheless, there still exist several battery systems capable of Al^{3+} intercalation. A key requirement for designing Al^{3+} instead of $AlCl_4^-$ intercalation is a more polarizable (softer) anionic structure for cathode materials to enable lower energy barrier for Al^{3+} ion transportation.

The study on Al^{3+}-based ITCs for RABs could date back to 2011. Archer et al reported V_2O_5 nanowires could enable reversible insertion/extraction of Al^{3+} in the RTIL electrolyte.[57] However, Menke and Reed pointed out that the stainless steel current collector used in Archer's work is not compatible with the electrolyte, leading to side reactions and capacity contribution in charge/discharge processes.[58] Thus, stainless steel may work as the active component instead of V_2O_5 nanowires. By replacing the stainless steel collector with Mo metal, Chiku's group again demonstrated the feasibility of V_2O_5 to act as RAB cathodes, evidenced by the reversible oxidation/reduction peaks from cyclic voltammetry (CV) curves and a reversible capacity of ~ 100 mAh g^{-1} in the 10th cycle.[59] Notably, this capacity is much lower than the V_2O_5 nanowires in Archer's work (305 mAh g^{-1}), indicating that the stainless steel indeed contributes to the capacity. Subsequent research was then focused on exploring new types of metal

DOI: 10.54227/mlab.20220055

Table 1. Electrochemical performances of reported RAB cathodes based on $AlCl_4^-$ intercalation.

Material	Discharge voltage (V)	Current density (A g^{-1})	Initial capacity (mAh g^{-1})	Final capacity (mAh g^{-1})	Cycle number
3D graphitic foam[16]	~ 2.0	4		60	7500
GA3000 graphene[35]	1.95	5	100	97	25000
GF-HC graphene[36]	~ 1.9	400	120	110	250000
3D graphene mesh[51]	~ 1.5	2.4	57	55	200
Graphene paper[52]	~ 1.5	1		~ 120	2800
Edge rich graphene[29]	~ 1.7	2	128	~ 90	20000
FLG graphene[41]	~ 1.7	1	173	100	55
graphene nanoribbon[30]	1.75	5	123	123	10000
graphite[53]	1.8	0.1		~ 70	100
NGF graphene[31]	~ 1.6	0.5	154	151	100
Natural graphite[40]	~ 1.7	0.66	60	60	6000
3DGF graphene[54]	~ 1.7	12	60	60	4000
Activated carbon[55]	---	1	~ 90		1500
PGN graphite[56]	~ 1.5	0.5	96	96	2000
SnS_2@G[42]	0.65	0.1	~ 275	70	100
SnS[43]	1.0	0.1	~ 400	227	100
$Cu_{2-x}Se$[44]	~ 0.5	0.2	241	100	100
SnSe[50]	~ 0.8	0.3	582	100	107
WO_{3-x}[45]	~ 1.0	0.1	~ 118	~ 64	100
WS_2[48]	0.7	1	250	119	500
NiTe[49]	~ 0.9	0.5	458	307	100
Cu_3P[47]	~ 0.8	0.05	73	17	50
$CoSe_2$[46]	1.2	2	400	125	1000

chalcogenides that could host Al^{3+}, such as VO_2[60], CuO[61], $MoSe_2$[62], Co_3O_4[63], Li_3VO_4[64], MnO_2[65], TiO2[66], MoS_2[67], etc. However, the experimental capacities of these current materials were out of satisfactory, showing the inferior rate and cycling performances.

Compositing metal chalcogenides with carbon was proved to be a feasible pathway to improve both cyclic stability and rate performance.[68–73] In metal chalcogenide/carbon hybrids, the carbon can not only function as physical support for metal chalcogenide to buffer its volume change during battery operation and protect active species from dissolution, but also enhance the charge/ion transport to facilitate the redox kinetics. Wang's group prepared a $CoSe_2$@carbon nanodice (C-ND) hybrid material to work as the cathode for RABs, exhibiting a high discharge capacity of 529 mAh g^{-1} at 1 A g^{-1}.[71] Unfortunately, the initial capacity decreases rapidly to 72 mAh g^{-1} after only 100 cycles. The authors suggested that a gradual dissolution of Co species into electrolyte and cathode pulverization occurs during repeated cycling, thus resulting in the rapid capacity loss (Fig. 7a). Based on this capacity deterioration mechanism, Wang's group further designed a $CoSe_2$/carbon nanodice/reduce graphene oxide ($CoSe_2$@C-ND@rGO) ternary composite material as the cathode, in which the rGO film could serve as a wrapping layer to protect the cathode materials from dissolution and pulverization (Fig. 7b). The $CoSe_2$@C-ND@rGO cathode shows better cycling stability than $CoSe_2$@C-ND, retaining a discharge capacity of 143 mAh g^{-1} after 500 cycles (Fig. 7c). Lu's group reported a free-standing MoS_2@carbon nanofiber composite cathode[72], exhibiting better rate and cycling performance (delivering an initial discharge capacity of 293 mAh g^{-1} at 100 mA g^{-1} and maintaining 126.6 mAh g^{-1} after 200 cycles.) than pristine MoS_2 cathode (delivering an initial discharge capacity of 253 mAh g^{-1} at 20 mA g^{-1} and maintaining 66 mAh g^{-1} after 100 cycles).

MXenes are the new class of cathode materials that can host the intercalation of Al^{3+} ions for RABs. Lukatskaya et al. developed a series of MXene materials that can accommodate a wide range of cations, including Al^{3+} ions.[74] Armin Vahid Mohammadi et al. recently reported the synthesis of vanadium carbide (V_2CT_x) MXene as the cathode material for RABs.[75] Few layered V_2CT_x MXene delaminated through the tetrabutylammonium hydroxide (TBAOH) intercalation can deliver a specific capacity of ~300 mAh g^{-1} at a current density of 0.1 A g^{-1}. However, MXene electrodes usually suffer from fast capacity attenuations, due to the strong electrostatic interaction between Al^{3+} ion and surface terminations (O, OH, and/or F groups) of MXene that hinders the reversible intercalation/deintercalation of Al^{3+} with high charge density. Therefore, it will be important to design MXene materials with relatively inert surface properties and large interlayer spacings for facilitating the Al^{3+} diffusion.

Prussian blue analogues represent metal-organic framework structures with the idealized formula of $A_xMFe(CN)_6{\cdot}yH_2O$, where A = Li, Na, Mg, Ca, etc. and M = Ba, Ti, Mn, Fe, Co, or Ni, that can store a wide range of ions.[76] Prussian blue analogues have been demonstrated as capable cathode materials for the reversible intercalation of multivalence metal ions including Al^{3+} in both aqueous and non-aqueous electrolyte systems with excellent electrochemical cyclabilities (2,000 cycles without obvious capacity fading). However, the insertion voltages (~0.60-1.3 V vs. SHE), as well as the specific capacities of 30-60 mAh/g of Prussian blue analogues, are far from satisfactory, resulting in relatively low energy densities of 102 Wh kg^{-1} and 171 Wh L^{-1}.[77] In summary, Al^{3+}-based ITCs normally possess a high initial specific capacity owing to the three-electron redox chemistry but are limited by low voltage and poor rate/cycling capabilities.

DOI: 10.54227/mlab.20220055

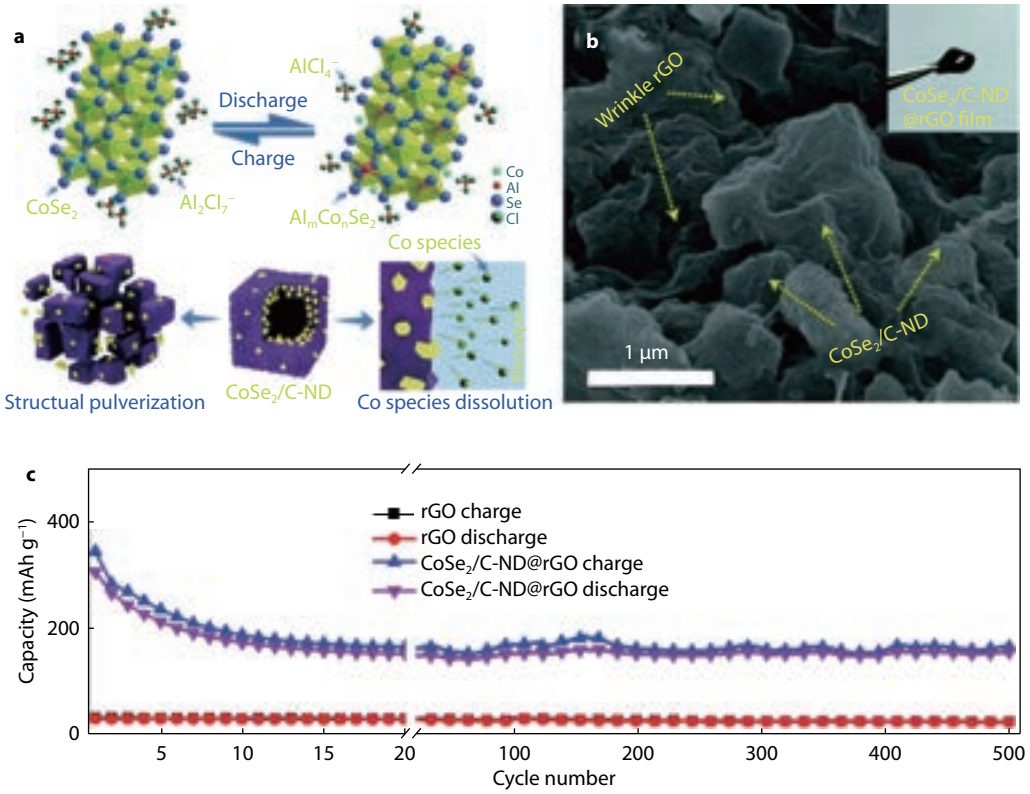

Fig. 7 **a** Schematic illustration of the energy storage (up) and capacity-deterioration (down) mechanisms for $CoSe_2$@C-ND cathode. **b** SEM images of $CoSe_2$@C-ND@rGO. **c** Cycling performance of $CoSe_2$@C-ND@rGO and rGO cathodes at the current density of 1 A g^{-1}.[71] Copyright 2018, Royal Society of Chemistry.

Conversion-type cathode

As electrodes in LIBs have developed from an intercalation mechanism to a conversion mechanism for higher energy density, the evolution of RAB cathodes follows the same path. The conversion-type cathode (CTC) has become a promising candidate to replace ITCs for AIBs, because of their high theoretical capacity and low cost. CTCs use active materials undergoing reversible electrochemical conversion reactions during battery operations. The conversion mechanism involves replacement reactions between charge carrier ions and electrode materials. Currently, CTCs are mostly based on chalcogens and metal chalcogenides.

Sulfur-based cathode

Among chalcogens, sulfur (S) was paid attention preferentially to work as RAB cathodes due to the incredible success of Li-S batteries. A CTC based on S could offer several advantages when coupling with the Al anode, in terms of earth abundance, low cost and high theoretical capacities (gravimetric capacity: 1672 mAh g^{-1} and volumetric capacity: 3459 mAh cm^{-3}).[78] The first non-aqueous Al-S battery cell was reported by Archer and co-workers in 2015.[79] The first-cycle discharge capacity of this battery is up to 1500 mAh g^{-1}, however, its rechargeability is extremely poor with a subsequent charge capacity of only around 300 mAh g^{-1}. Through encapsulating S into activated microporous carbons, Wang's group fabricated the first reversible Al-S battery in RTIL electrolytes.[80] The improved reversibility is largely attributed to the confinement of S and its reduced product (AlS_x) in the micropores, facilitating the AlS_x oxidation kinetics. Such an Al-S@C battery shows a discharge voltage of ~ 0.65 V and a specific capacity of 1320 mAh g^{-1} at 50 mA g^{-1} (Fig. 8a). Although the rechargeability of Al-S batteries has been settled, it can only operate for 20 cycles (Fig. 8b). People then turned to study the working mechanism of Al-S batteries, aiming to understand the underlying reasons for their inferior voltage and cyclability. Manthiram and co-workers suggested that the electrochemical reduction of S upon discharging involves the formation of both sulfide and polysulfides (Fig. 8c).[81,82] After further analyzing electrochemical, microscopic and spectroscopic results, they demonstrated that long-chain polysulfides (S_x^{2-}, $x \geq 6$) are soluble in the electrolyte, while short-chain polysulfides (S_x^{2-}, $1 \leq x < 6$) are insoluble (Fig. 8d). The insoluble and insulating nature of final products of S cathode leads to sluggish reaction kinetics, thus reducing the reversible capacity, rate capability and cycling stability.

Currently, the research focusing on S-based cathode is exploring functionalized carbon hosts.[83–86] Ji et al anchored S on a copper (Cu)-doped carbon matrix to prepare a S@HKUST-1-C composite cathode (Fig. 8e).[84] The S@HKUST-1-C cathode showed a reversible capacity of 600 mAh g^{-1} at 1 A g^{-1} and maintained at 460 mAh g^{-1} after 500 cycles (Fig. 8f). The improved electrochemical performance can be explained by the two positive effects of Cu. Cu not only forms ionic clusters with AlS_x that facilitate redox kinetics but also increases the electrical conductivity at S@HKUST-1-C interfaces and decreases the kinetic barriers of S/AlS_x conversion.

DOI: 10.54227/mlab.20220055

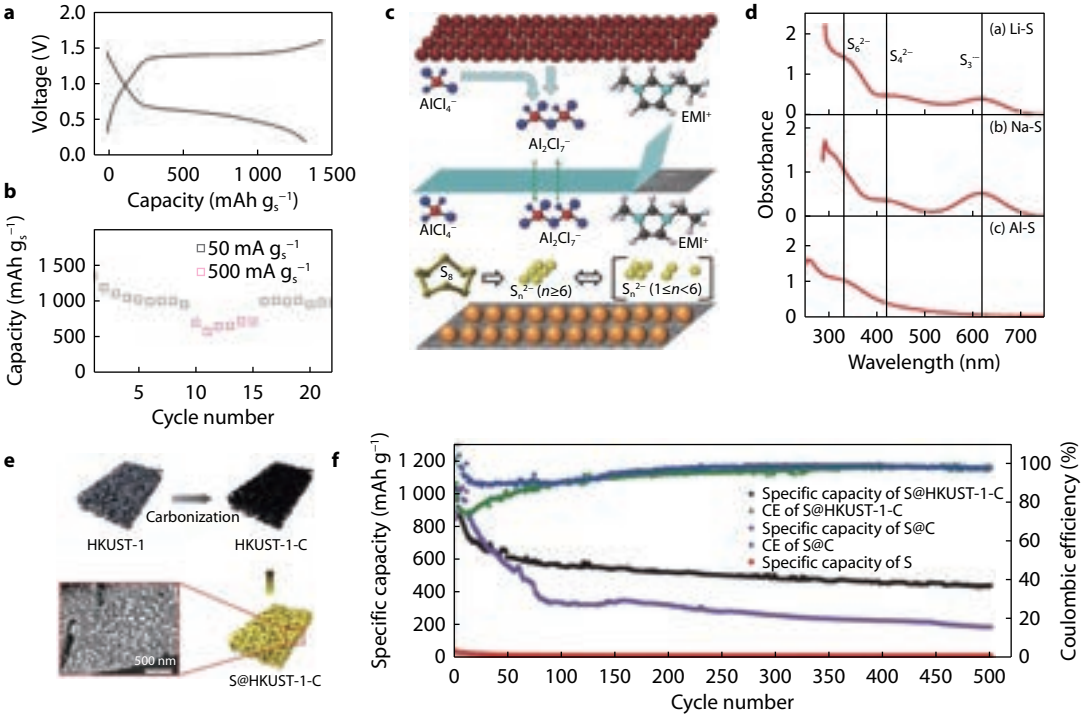

Fig. 8 **a** A typical charge-discharge curves and **b** cycling stability of the Al-S battery with S@microporous carbon cathode.[80] Copyright 2016, Wiley-VCH Verlag GmbH & Co. **c** Schematic illustration of the charge-discharge mechanism of the Al-S battery.[82] Copyright 2017, Wiley-VCH Verlag GmbH & Co. **d** UV-vs spectra of the S cathodes discharged in Li-S, Na-S and Al-S batteries.[81] Copyright 2018, Cell Press. **e** Schematic illustration of the preparation of S@HKUST-10C. **f** Cycling performance of S@HKUST-10C, S@C, and S under 1 A g^{-1}.[84] Copyright 2019, Wiley-VCH Verlag GmbH & Co.

A similar metal incorporation strategy was reported by Guo and co-workers.[85] Benefiting from the catalytic effect of cobalt (Co) embedded in the carbon host, their Al-S battery maintained a specific capacity of ~ 500 mAh g^{-1} after 200 cycles at the current density of 1 A g^{-1}. Besides metal doping, nitrogen (N)-doped carbon host (HPCK) was studied for Al-S batteries very recently. Yu et al designed an N-doped porous carbon host simultaneously possessing a high surface area (2513 m^2 g^{-1}) and hierarchical macro-, meso- and micropores.[83] The hierarchical structure provides fast ion transport channels and stable accommodation of S, while the N-doped carbon matrix anchors sulfide and polysulfide intermediates. The S@HPCK cathode showed good cycling stability, with a capacity of 405 mAh g^{-1} after 700 cycles at 1 A g^{-1}.

As summarized in Table 2, S@C composite cathodes generally hold high reversible specific capacities (400~500 mAh g^{-1}) owing to the light molecular weight and multi-electron transfer of S. Although the rate/cycling capabilities can be improved by structural or compositional modification of carbon host materials, discharge voltages of current Al-S batteries are extremely low (< 0.7 V), hindering its further development. Qiao's group proposed a sulfur oxidation mechanism in the $AlCl_3$/urea electrolyte very recently, exhibiting a high discharge voltage of ~ 1.8 V. Nonetheless, this novel concept is in the early stage, and still needs further studies to prove its potential. Exploring alternative chalcogens with high discharge voltage is a more readily way.

Selenium-based cathode

Selenium (Se), as a chemical analogue to S, has been proven to be an emerging cathode material for RABs. Different from S cathode, Se cathode undergoes an electrochemical oxidation process owing to its lower ionization potential (Se: 9.7 eV vs. S: 10.4 eV)[87–90], consequently displaying a higher discharge voltage. Besides, the higher conductivity of Se (1×10^{-3} S m^{-1}) over S (5×10^{-28} S m^{-1}) is another merit for its use in RABs with improved rate capabilities. Huang et al designed an Al-Se battery prototype in 2018, consisting of a composite cathode containing Se nanowires and mesoporous carbon nanorods (CMK-3), an Al metal anode and RTIL ($AlCl_3$/[EMIm]Cl) electrolyte.[91] The working mechanism of this battery is demonstrated to be the reversible redox reaction of the Se/Se_2Cl_2 pair confined in the carbon mesopores of CMK-3 (Fig. 9a). The Se@CMK-3 cathode delivers a high reversible capacity of 178 mAh g^{-1} at 100 mA g^{-1} with high discharge voltage (> 1.5 V).

Subsequently, several research groups claimed that Se could be oxidized to form not only Se_2^{2+} but also Se^{2+}, Se^{4+} and Se^{6+}, contributing to greatly increased capacities.[92–95] Li's group prepared a hollow Se@carbon nanotube (Se@CT) to work as a composite cathode for AIBs, delivering a discharge voltage of ~ 1.6 V and specific capacities of 422, 305, 212, 173 mAh g^{-1} at current densities of 0.2, 0.3, 0.4 and 0.5 A g^{-1}, respectively.[93] The capacity still maintains 163 mAh g^{-1} at 0.5 mA g^{-1} after 200 cycles. XPS results of Se@CT cathode at fully charged and fully discharged states confirmed the existence of Se^{2+} and Se^{4+} after charging, which explains its higher specific capacities than that of Se@CMK-3 cathode. Jiao group claimed $SeCl_4$ as the charge product, affording for a four-electron transfer mechanism (Fig. 9b).[92] With the CMK-3 modi-

DOI: 10.54227/mlab.20220055

Table 2. electrochemical performance of S@C composite cathodes for RABs.

Material	Discharge voltage (V)	Current density (mA g^{-1})	Initial capacity (mAh g^{-1})	Final capacity (mAh g^{-1})	Cycle number
S@ACC[80]	0.65	50	1320	1000	20
S@HPCK[83]	~0.6	1000	530	405	700
S@HKUST-1-C[84]	0.4	1000	~1050	460	500
S@Co@C[85]	~0.6	1000	1650	~500	200

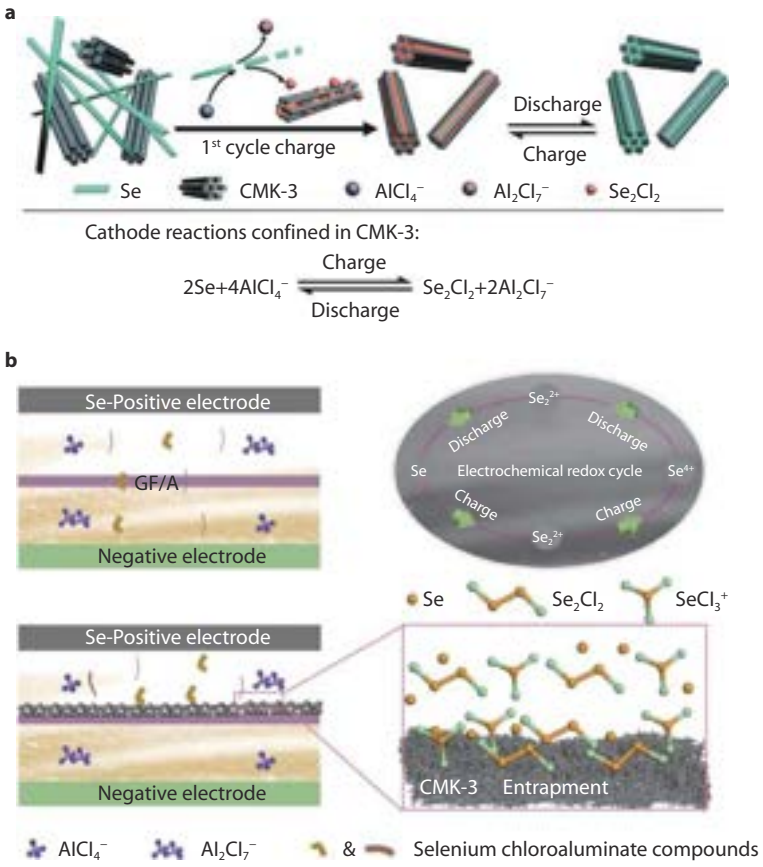

Fig. 9 **a** Schematic illustration of the proposed mechanism of Al-Se batteries using Se nanowires and CMK-3 composite cathodes, and reversible reaction of the Se cathode.[91] Copyright 2018, Royal Society of Chemistry. **b** The schematic diagram of the redox cycle process of Se cathode.[92] Copyright 2020, Elsevier.

fied separator, Se cathode in this work showed a discharge voltage of 1.5 V and an initial capacity of 1009 mAh g^{-1} at 1 A g^{-1}. However, the capacity decayed rapidly in the first 50 cycles and retained 270 mAh g^{-1} after 500 cycles, which is largely attributed to the dissolution of products during battery operation. Recently, Yan et al. proposed a six-electron reaction process ($Se^{2-} \leftrightarrow Se \leftrightarrow Se^{4+}$) of selenim@graphene aerogel (Se@GA) cathode in $AlCl_3$/Et_3NHCl RTIL electrolyte.[95] With the carbon-modified separator to further prevent shuttling effects, the Se@GA cathode delivered high specific capacities of 1599 and 580 mAh g^{-1} at 0.1 and 1 A g^{-1}, respectively. Furthermore, outstanding cycling performance was observed with capacity retention of 395 mAh g^{-1} at 1 A g^{-1} after 500 cycles.

Compared with S, Se is more promising as RAB cathodes because it can afford a high working voltage (>1.5 V). However, Se cathode still faces general problems of conversion reactions such as shuttling effect, structural collapse and volume expansion. Therefore, Se materials need to be encapsulated into host materials commonly carbonaceous materials. The structure and composition of host materials hold the key for the development of Se cathode for RABs.

Others

Tellurium (Te) is known to have the highest electrical conductivity (2×10^{-4} S m^{-1})[96] among chalcogens, thus allowing for good rate performance of the Al-Te battery. Different from S and Se cathodes mentioned above, Te cathode can be prepared by directly coating the slurry of Te powder, carbon additives and binder on the current collector without using host materials.[97] The assembled Al-Te battery is demonstrated to be reversible with a high capacity of 913 mAh g^{-1} and an obvious discharge voltage of ~ 1.5 V, based on the reversible transformation of Te to Te^{2-}/$TeCl^{3+}$ (Fig. 10). However, its long-term cycling is still hindered by rapid capacity fading, coming from the production of soluble tellurium chloroaluminate compounds upon charging. Jiao and co-workers modified the cell configuration, using rGO to support Te cathode

DOI: 10.54227/mlab.20220055

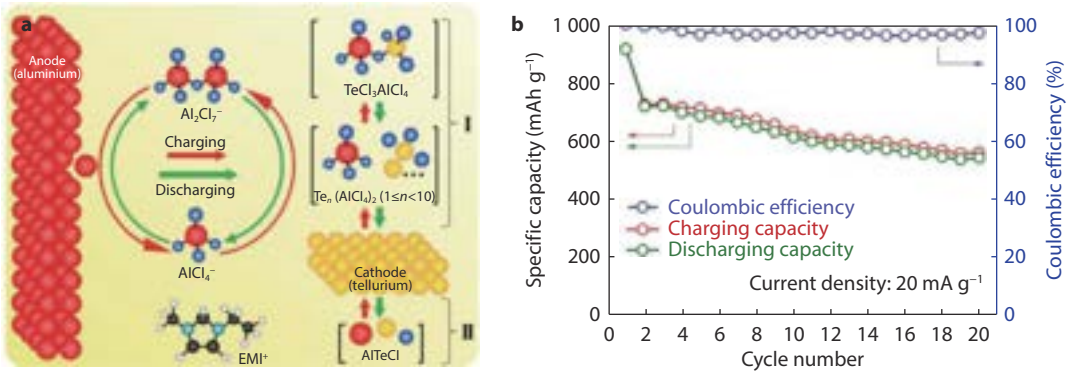

Fig. 10 **a** Working mechanism and **b** cyclic stability of an Al-Te cell.[97] Copyright 2018, American Chemical Society.

and SWCNT to functionalize the separator, aiming to suppress the shuttling effects.[98] This Te@rGO cathode delivered a discharge capacity of ~1026 mAh g^{-1} at 0.5 A g^{-1} with a discharge voltage of 1.4 V. The capacity still maintained ~ 480 mAh g^{-1} after 100 cycles at the current density of 1 A g^{-1}. The same research group further applied N-doped porous carbon (N-PC) to act as an effective Te host.[99] Such Te@N-PC exhibited improved long-term cycling capability at 0.5 A g^{-1}, with 467 mAh g^{-1} capacity retention after 150 cycles.

In addition to chalcogens, metal chalcogenides were adopted as CTCs in RABs, such as FeS_2[100,101], Co_9S_8[102], CoS_2[103], CuS[104], CuNiS[105], Cu_xSe[106], $CoSe_2$[107,108], $MoSe_2$[62], Sb_2Se_3[109], Bi_2Te_3[110] etc. The chalcogen elements in these materials are responsible for the majority of their capacities, while the metal atoms enhance the overall electrical conductivity for fast kinetics and provide polarity for binding soluble polysulfide/polyselenide intermediates. Similar to chalcogens, metal chalcogenides working with a conversion reaction mechanism also suffer from great volume expansion and shuttling effect, resulting in poor cyclic performance. For example, Wang's group designed a free-standing Co_9S_8@CNTs-CNFs composite cathode for RABs.[102] Although this cathode exhibited a high initial capacity of 315 mAh g^{-1} at 100 mA g^{-1}, it could only maintain 87 mAh g^{-1} after 6000 cycles at 1 A g^{-1}. The same cycling issue also happened in metal selenide cathodes. Yu et al embedded $CoSe_2$ particles into an N-doped porous carbon nanosheets ($CoSe_2$@NPCS) to form a composite cathode for RABs. The $CoSe_2$@NPCS cathode exhibited an initial discharge capacity of 436 mAh g^{-1} at 1 A g^{-1} with only less than 50% capacity retention after 500 cycles.

Coordination-type cathode

Recently, the choice of cathode materials for RABs has been expanded to organic molecules owing to their availability of flexible intermolecular spaces, which can be utilized for the diffusion and storage of bulky aluminium complex ions. In addition, organic molecules are also chemically and structurally diverse and can be functionally tailored to suit the needs of RAB cathodes. Up to now, several organic cathodes (OCs) have been reported for RABs, including phenantherenequinone (PQ)[111], polyaniline (PANI)[112] polypyrene[113], porphyrin[114], poly (nitropyrene-co-pyrene)[113], tetradiketone (TDK)[115] and anthraquinone (AQ)[116]. Normally, organic electrodes are classified into n-type and p-type depending on their charge states during redox reactions.

In RABs, n-type OCs form anions during discharging to combine with positive counterions from the electrolyte. This type of OCs generally contains C=O or C=N active sites to coordinate with positively charged carriers, such as $AlCl_2^+$ and $AlCl^{2+}$,[111,115] resulting in fast reaction kinetics in electrochemical processes. Unfortunately, small organic molecules suffer from poor electrical conductivity and serious dissolution into the electrolyte, thus limiting their electrochemical performances. Stoddart et al. designed a PQ-based triangular macrocycle (PQ-Δ) as the cathode for AIBs (Fig. 11a).[111] This architecture could not only prevent the dissolution of organic molecules into the electrolyte but also form layered structures for $AlCl_2^+$ insertion and extraction during battery cycling (Fig. 11a). The PQ-Δ cathode exhibited a discharge voltage of ~1.2 V, a reversible capacity of 110 mAh g^{-1}, and superior cyclability of up to 5000 cycles.

Choi and coworkers also designed a macrocycle based on tetradiketone (TDK).[115] Different from previous reports, they proved that the TDK cathode could reversibly coordinate with divalent ($AlCl^{2+}$) ions (Fig. 11b), eventually achieving a high specific capacity of 350 mAh g^{-1} at a very low current density of 20 mA g^{-1}. Long-term cycling results showed a reversible capacity of around 170 mAh g^{-1} for 300 cycles at 0.1 A g^{-1}. Another method is to use polymers as the OC. Compared with organic molecules, their polymeric counterparts have better chemical stability and electrical conductivity due to their long-range conjugated structures and conjugated chemical bonds. However, the number of active sites is relatively lower in polymers. With these considerations, Niu et al. fabricated a protonated PANI@SWCNT composite OC in AIBs.[113] The protonation treatment is demonstrated to endow more active sites for coordinating $AlCl_2^+$ ions (Fig. 11c) and improve the conductivity of PANI. As a result, the protonated PANI@SWCNT cathode delivered a high specific capacity of ~ 200 mAh g^{-1}[112], which is twice as high as that of the non-protonated counterpart (Fig. 11d). Moreover, remarkable rate/cycling performance was observed, with a reversible capacity of around 100 mAh g^{-1} at a high current density of 10 A g^{-1} for 8000 cycles.

As an alternative, p-type OCs, commonly polycyclic hydrocarbons (PAHs), undergo oxidation and bind negatively charged carrier ($AlCl_4^-$) during discharging (Fig. 12a). Polypyrene was the first p-type OC for AIBs, reported by Kovalenko et al.[113] in 2018. They used the polypyrene as OC, exhibiting a high discharge voltage of ~1.7 V and a reversible

DOI: 10.54227/mlab.20220055

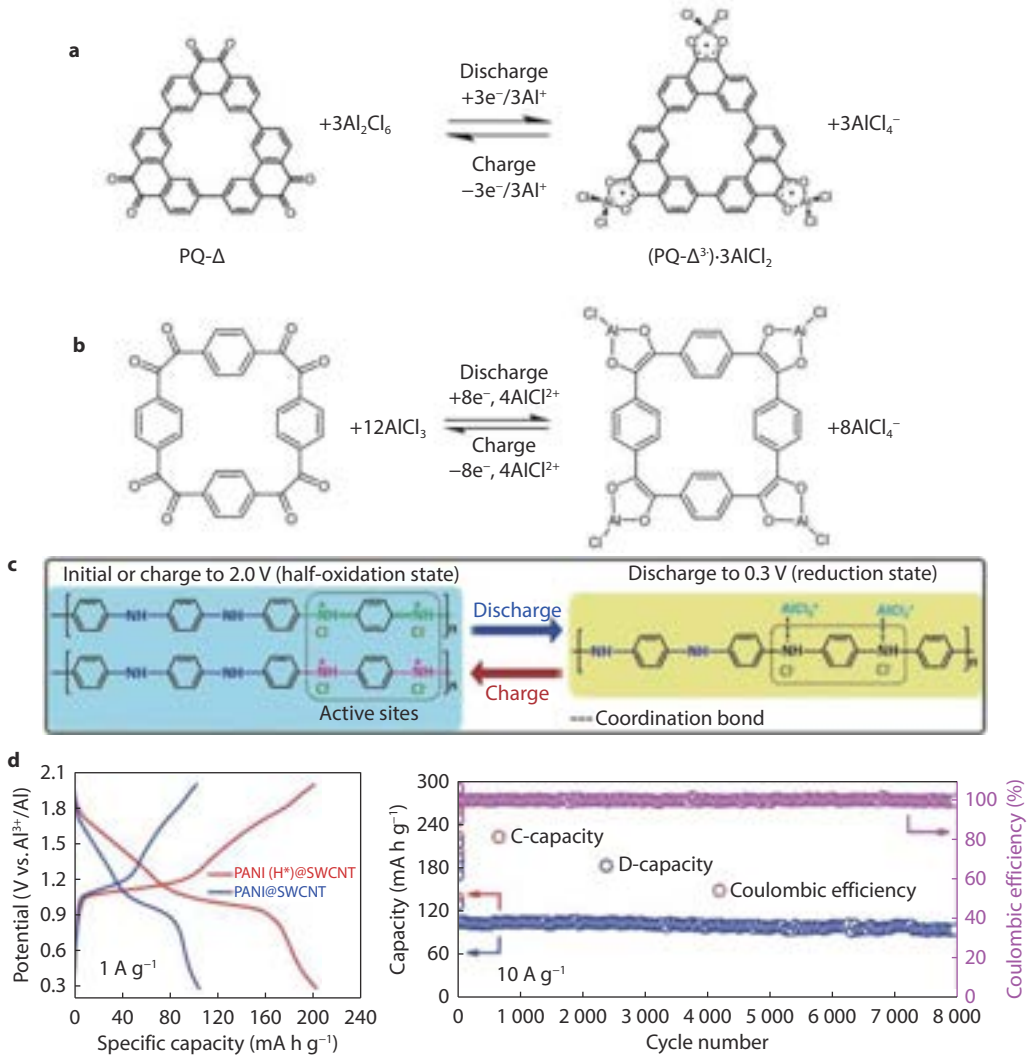

Fig. 11 **a** Electrochemical redox chemistry of PQ-Δ cathode.[111] Copyright 2019, Nature Publishing Group. **b** Electrochemical redox mechanism of TDK cathode.[115] Copyright 2021, Nature Publishing Group. **c** Electrochemical redox mechanism and **d** charge-discharge curves and cycling stability of PANI (H^+)@AWCNT cathode.[112] Copyright 2020, Wiley-VCH Verlag GmbH & Co.

capacity of 70 mAh g^{-1}, higher than the crystalline pyrene (20 mAh g^{-1}) (Fig. 12b). Subsequently, Xing and co-workers evaluated the potential of a series of PAHs using first-principles calculations, including coronene ($C_{24}H_{12}$), perylene ($C_{20}H_{12}$), pyrene ($C_{16}H_{10}$), anthracene ($C_{14}H_{10}$), naphthalene ($C_{10}H_8$) and benzene (C_6H_6).[117] They suggested a negative correlation between the theoretical capacity of PAHs and their number of aromatic rings. Guided by the calculation results, they employed these PAHs as AIB cathodes in practical. It is demonstrated that C_6H_6, with three aromatic rings, showed the highest specific capacity (157 mAh g^{-1}) at 100 mA g^{-1} and maintained at 130 mAh g^{-1} after 800 cycles.

Reported OCs were listed in Table 3 and their electrochemical performances are presented. In general, n-type OCs can deliver good reversible capacities, but limited by low discharge voltage (1.0-1.2 V). Compared to n-type OCs, p-type OCs displayed high voltages (>1.5 V), which is more favorable for high-performance AIBs. Nevertheless, their specific capacities are limited. It remains a challenge for current OCs to provide both high voltage and high capacity.

Conclusions and outlook

RABs have exhibited advantages of resource abundance and high safety over the state-of-the-art LIBs, and become one of the promising post-LIB candidates. A broad range of available RAB cathode materials have been developed for this purpose. GCs, in particular graphene, hold a great potential working as the RAB cathode due to their high operating voltage, fast charge-discharge property, and long cycle life. Although research progress in this front is remarkable, current graphene cathodes for RABs are still limited by their low capacities (~ 60-170 mAh g^{-1}). Based on the fundamental science acquired from previous reports, the ideal RAB graphene cathodes should satisfy requirements from aspects of morphology, structure and composition. Specifically, the graphene cathode should possess 1) few-layer structure to afford flexibility and mechanical strength for fast kinetics of $AlCl_4^-$ insertion/extraction; 2) sufficient active sites (either from edges or basal planes) to provide express pathways for $AlCl_4^-$ ions; 3) high quality with no heteroatoms and functional

DOI: 10.54227/mlab.20220055

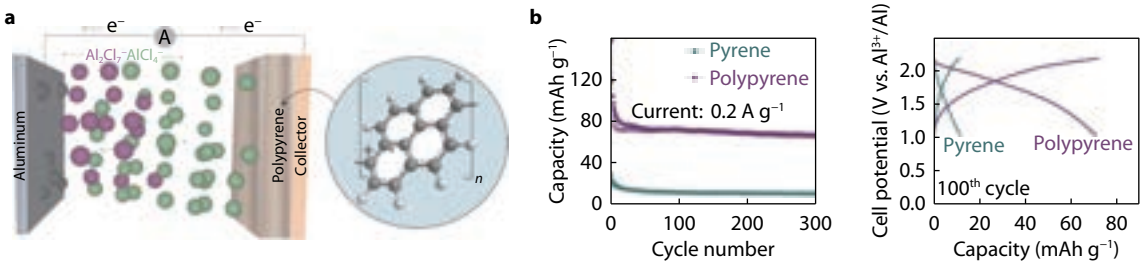

Fig. 12 **a** Working mechanism of a RAB cell during charging with a polypyrene cathode. **b** Electrochemical performance of RABs with polypyrene and pyrene as cathodes.[113] Copyright 2020, Wiley-VCH Verlag GmbH & Co.

Table 3. Electrochemical performance of current OCs in RABs.

Material	Discharge voltage (V)	Current density (A g^{-1})	Initial capacity (mAh g^{-1})	Final capacity (mAh g^{-1})	Cycle number
Phenanthrenequinone[111]	~ 1.2	2	90	50	5000
Tetradiketone[115]	~ 1.2	0.1	~ 230	~ 170	300
Porphyrin[114]	---	0.2	~ 85	~ 75	5000
Anthraquinone[116]	~ 1.0		160	120	500
Polyaniline[112]	~ 1.0	10	100	100	8000
Polypyrene[113]	~ 1.7	0.2	~ 95	70	300
Poly (nitropyrene-co-pyrene)[113]	~ 1.7	0.2	~ 110	~ 80	1000
Anthracene[117]	~ 1.6	0.1	157	130	800

groups to avoid side reactions and supercapacitive behaviour; 4) expanded interlayer space to accommodate large-size $AlCl_4^-$ ions; 5) economic preparation method to provide opportunities for scalable production. It can be expected that simultaneously fulfilling the above-mentioned requirements hold great promise towards high-capacity and low-cost graphene cathodes for RABs. Unfortunately, current graphene processing methods failed to realize this delicate design. Hence, more efforts should be paid in this aspect.

Furthermore, the Se cathode is also a promising candidate because of its high theoretical capacity and high voltage (> 1.5 V). Currently, Al-Se batteries can deliver high initial capacities, but decay rapidly in the first tens of cycles, leading to inferior reversible capacities. This is mainly ascribed to the continuous dissolution of Se and polyselenide intermediates and slow redox kinetics during charging and discharging. Mesoporous carbons have made remarkable contributions to Al-Se batteries, due to their ability to confine Se species and enhance electrical conductivity during charging and discharging processes. Previous studies on Se-based RAB cathodes mainly focused on their working mechanisms, but lacked rational design of mesoporous carbon host materials. Ideal host materials for Al-Se batteries should possess high surface area, good conductivity and suitable mesopore geometry. Therefore, more attention should be given to such research.

In the aspect of OCs, p-type OCs are more favorable to be utilized in RABs because of their high redox voltages (> 1.5 V). However, previously reported p-type OCs, can only deliver limited specific capacity (70-150 mAh g^{-1}), due to their intrinsic one-electron reaction mechanism. According to Faraday's law, if increasing the electron transfer number of a certain p-type OC, the theoretical capacity would be remarkably improved. Generally, p-type OCs develop single charged radical intermediates (SCRIs) during charging followed by reacting with $AlCl_4^-$ ions, which is an energy-consuming process. Further generation of multiple charged radical intermediates (MCRIs) requires more energy and thus occurs at a higher potential than SCRIs. However, the voltage threshold of $AlCl_3$/[EMIm]Cl electrolyte is limited (~2.3 V), making p-type OC cathodes very difficult to form MCRIs in AIBs during charging. As a result, enabling multi-redox chemistry of p-type OCs is still of great challenge. Grafting electron-donating substitutes at organic compounds has been reported as an effective strategy to promote electron transfer in applications such as redox flow batteries. The feasibility of this strategy for p-type OCs in RABs should be evaluated for the capacity improvement. The n-type OC with multiple active units (C=O, C=N…) offer multi-electron transfer but suffer from low working voltage. However, previous work only focused on demonstrating the feasibility of various high-capacity n-OCs, in-depth investigation of high-voltage design is overlooked. Increasing the coordination affinity between n-OCs and chloroaluminate ions through designing the structure and distribution of active units could potentially improve the voltage profile. Moreover, small organic molecules have high solubility in the electrolyte, leading to low cycling stability. The selection and design of the proper molecular structure of OCs and electrode modification approaches are eagerly explored to construct green, sustainable and high-performance OCs for RABs.

Another two perspectives can be considered at the RAB configuration level. (1) The fundamental chemistry of Al stripping/plating in current non-aqueous RTIL electrolytes requires a large amount of electrolyte, significantly reducing the energy density of a whole RAB cell. In addition, the RTILs are expensive and need highly specialized cell materials (e.g., Ta, Mo) to avoid corrosion. Therefore, exploring more suitable electrolyte systems is desirable for the development of RABs. (2) To accelerate the practical use of RABs, researchers should pay attention not only to the cathode materials and their electrochemistry but also to the battery configuration design. For instance, the currently used glass fibre separator has a high price, high thickness and poor mechanical properties. Therefore, cost-effective substitutes with flexible, thin,

DOI: 10.54227/mlab.20220055

and anti-corrosive features are favorable in RABs, which is worth studying.

■ ACKNOWLEDGEMENTS

We acknowledge the support from Australian Research Council, Queensland Government, China Scholarship Council and the University of Queensland.

■ CONFLICT OF INTEREST

The authors declare no conflict of interest.

■ AUTHOR CONTRIBUTIONS

Y. Q. K., X. D. H. and A. K. N. wrote this review. N. A. G., S. M. C., D. R. and C. Z. Y. helped with the manuscript revision.

■ REFERENCES

1. M. Allen, M. Babiker, Y. Chen and H. C. de Coninck, IPCC Special Report Global Warming of 1.5 °C , Intergovernmental Panel on Climate Change, 2018.
2. IEA, Net Zero by 2050, Paris. https://www.iea.org/reports/net-zero-by-2050, May 2021.
3. M. Li, J. Lu, Z. Chen and K. Amine, *Adv. Mater.*, 2018, 30, 1800561
4. G. E. Blomgren, *J. Electrochem. Soc.*, 2016, 164, A5019
5. N. Nitta, F. Wu, J. T. Lee and G. Yushin, *Mater. Today*, 2015, 18, 252
6. V. Etacheri, R. Marom, R. Elazari, G. Salitra and D. Aurbach, *Energy Environ. Sci.*, 2011, 4, 3243
7. R. Sun, S. Dong, F. Xu, Z. Li, C. Wang, S. Lu and H. Fan, *Dalton Trans.*, 2022, 51, 7607
8. X. Guo, W. Zhang, J. Shi, M. Duan, S. Liu, J. Zhang, Y. Liu, S. Xiong and Q. Kong, *Nano Res.*, 2022, 15, 3, 2092
9. Z. Li, Z. Peng, R. Sui, Z. Qin, X. Liu. C. Wang, H. Fan and S. Lu, *Chi. J. Chem.*, 2021, 39, 2599
10. Z. Gu, J. Guo, Z. Sun, X. Zhao, X. Wang, H. Liang, X. Wu and Y. Liu, *Cell Rep. Phys. Sci.*, 2021, 2, 100665
11. Y. Heng, Z. Gu, J. Guo and X. Wu, *Acta. Phys. Chim. Sin.*, 2021, 37, 2005013
12. J. Tu, W.-L. Song, H. Lei, Z. Yu, L.-L. Chen, M. Wang and S. Jiao, *Chem. Rev.*, 2021, 121, 4903
13. E. Faegh, B. Ng, D. Hayman and W. E. Mustain, *Nat. Energy*, 2021, 6, 21
14. H. Yang, H. Li, J. Li, Z. Sun, K. He, H. M. Cheng and F. Li, *Angew. Chem. Int. Ed.*, 2019, 58, 11978
15. F. Wu, H. Yang, Y. Bai and C. Wu, *Adv. Mater.*, 2019, 31, 1806510
16. M.-C. Lin, M. Gong, B. A. Lu, Y. P. Wu, D.-Y. Wang, M. Y. Guan, M. Angell, C. X. Chen, J. Yang, B.-J. Hwang and H. J. Dai, *Nature*, 2015, 520, 324
17. D. Tommasi, Traité des piles électriques: piles hydro-électriques accumulateurs, piles thermo-électriques et pyro-électriques, George Carré, 1889.
18. G. W. Heise, E. A. Schumacher and N. Cahoon, *J. Electrochem. Soc.*, 1948, 94, 99
19. Sargent, D. E. Voltaic Cell. US Patent 2554447, 1951.
20. S. Zaromb, *J. Electrochem. Soc.*, 1962, 109, 1125
21. B. S. Del Duca, *J. Electrochem. Soc.*, 1971, 118, 405
22. P. Rolland and G. Mamantov, *J. Electrochem. Soc.*, 1976, 123, 1299
23. N. Koura, *J. Electrochem. Soc.*, 1980, 127, 1529
24. N. Takami and N. Koura, *J. Electrochem. Soc.*, 1989, 136, 730
25. Q.-X. Qin and M. Skyllas-Kazacos, *J. Electroanal. Chem. Interfacial Electrochem.*, 1984, 168, 193
26. C. Dymek, J. Williams, D. Groeger and J. Auborn, *J. Electrochem. Soc.*, 1984, 131, 2887
27. M. P. Paranthaman, G. Brown, X.-G. Sun, J. Nanda, A. Manthiram and A. Manivannan, in ECS Meeting Abstracts, IOP Publishing, 2010.
28. L. Shen, X. Du, M. Ma, S. Wang, S. Huang and L. Xiong, *Adv. Sustain. Syst.*, 2022, 6, 2100418
29. Q. F. Zhang, L. L. Wang, J. Wang, C. Y. Xing, J. M. Ge, L. Fan, Z. M. Liu, X. L. Lu, M. G. Wu, X. Z. Yu, H. Zhang and B. A. Lu, *Energy Stor. Mater.*, 2018, 15, 361
30. X. Yu, B. Wang, D. Gong, Z. Xu and B. Lu, *Adv. Mater.*, 2017, 29, 1604118
31. X. Huang, Y. Liu, H. Zhang, J. Zhang, O. Noonan and C. Yu, *J. Mater. Chem. A*, 2017, 5, 19416
32. Z. Chen, W. Ren, L. Gao, B. Liu, S. Pei and H.-M. Cheng, *Nat. Mater.*, 2011, 10, 424
33. L. Zhang, L. Chen, H. Luo, X. Zhou and Z. Liu, *Adv. Energy Mater.*, 2017, 7, 1700034
34. A. S. Childress, P. Parajuli, J. Zhu, R. Podila and A. M. Rao, *Nano Energy*, 2017, 39, 69
35. H. Chen, F. Guo, Y. Liu, T. Huang, B. Zheng, N. Ananth, Z. Xu, W. Gao and C. Gao, *Adv. Mater.*, 2017, 29, 1605958
36. H. Chen, H. Y. Xu, S. Y. Wang, T. Q. Huang, J. B. Xi, S. Y. Cai, F. Guo, Z. Xu, W. W. Gao and C. Gao, *Sci. Adv.*, 2017, 3, eaao7233
37. A. Childress, P. Parajuli, S. Eyley, W. Thielemans, R. Podila and A. M. Rao, *Chem. Phys. Lett.*, 2019, 733, 136669
38. H. Huang, F. Zhou, X. Shi, J. Qin, Z. Zhang, X. Bao and Z.-S. Wu, *Energy Stor. Mater.*, 2019, 23, 664
39. J. Smajic, A. Alazmi, N. Batra, T. Palanisamy, D. H. Anjum and P. M. Costa, *Small*, 2018, 14, 1803584
40. D.-Y. Wang, C.-Y. Wei, M.-C. Lin, C.-J. Pan, H.-L. Chou, H.-A. Chen, M. Gong, Y. P. Wu, C. Z. Yuan, M. Angell, Y.-J. Hsieh, Y.-H. Chen, C.-Y. Wen, C.-W. Chen, B.-J. Hwang, C.-C. Chen and H. J. Dai, *Nat. Commun.*, 2017, 8, 14283
41. H. Huang, F. Zhou, P. Lu, X. Li, P. Das, X. Feng, K. Müllen and Z.-S. Wu, *Energy Stor. Mater.*, 2020, 27, 396
42. Y. Hu, B. Luo, D. Ye, X. Zhu, M. Lyu and L. Wang, *Adv. Mater.*, 2017, 29, 1606132
43. K. Liang, L. Ju, S. Koul, A. Kushima and Y. Yang, *Adv. Energy Mater.*, 2019, 9, 1802543
44. J. Jiang, H. Li, T. Fu, B.-J. Hwang, X. Li and J. Zhao, *ACS Appl. Mater. Interfaces*, 2018, 10, 17942
45. J. Tu, H. Lei, Z. Yu and S. Jiao, *Chem. Commun.*, 2018, 54, 1343
46. H. Hong, J. Liu, H. Huang, C. Atangana Etogo, X. Yang, B. Guan and L. Zhang, *J. Am. Chem. Soc.*, 2019, 141, 14764
47. G. Li, J. Tu, M. Wang and S. Jiao, *J. Mater. Chem. A*, 2019, 7, 8368
48. Z. Zhao, Z. Hu, Q. Li, H. Li, X. Zhang, Y. Zhuang, F. Wang and G. Yu, *Nano Today*, 2020, 32, 100870
49. Z. Yu, S. Jiao, J. Tu, Y. Luo, W.-L. Song, H. Jiao, M. Wang, H. Chen and D. Fang, *ACS Nano*, 2020, 14, 3469
50. Y. Zhang, B. Zhang, J. Li, J. Liu, X. Huo and F. Kang, *Chem. Eng. J.*, 2021, 403, 126377
51. G. Yang, L. Chen, P. Jiang, Z. Guo, W. Wang and Z. Liu, *RSC Adv.*, 2016, 6, 47655
52. P. Wang, H. Chen, N. Li, X. Zhang, S. Jiao, W.-L. Song and D. Fang, *Energy Stor. Mater.*, 2018, 13, 103
53. H. Sun, W. Wang, Z. Yu, Y. Yuan, S. Wang and S. Jiao, *Chem. Commun.*, 2015, 51, 11892
54. Y. P. Wu, M. Gong, M.-C. Lin, C. Z. Yuan, M. Angell, L. Huang, D.-Y. Wang, X. D. Zhang, J. Yang, B.-J. Hwang and H. J. Dai, *Adv. Mater.*, 2016, 28, 9218
55. P. Thanwisai, N. Chaiyapo, P. Phuenhinlad, Y. Kanaphan, J. Nash,

DOI: 10.54227/mlab.20220055

C. Chotsuwan, A. Klamchuen, Y. Wang, T. Nann and N. Meethong, *Carbon*, 2022, 191, 195
56. J. Yu, X. Li, N. Li, T. Wu, Y. Liu, C. Li, J. Liu and L. Wang, *Small Methods*, 2022, 6, 2200026
57. N. Jayaprakash, S. Das and L. Archer, *Chem. Commun.*, 2011, 47, 12610
58. L. D. Reed and E. Menke, *J. Electrochem. Soc.*, 2013, 160, A915
59. M. Chiku, H. Takeda, S. Matsumura, E. Higuchi and H. Inoue, *ACS Appl. Mater. Interfaces*, 2015, 7, 24385
60. W. Wang, B. Jiang, W. Y. Xiong, H. Sun, Z. S. Lin, L. W. Hu, J. G. Tu, J. G. Hou, H. M. Zhu and S. Q. Jiao, *Sci. Rep.*, 2013, 3, 3383
61. X. Zhang, G. Zhang, S. Wang, S. Li and S. Jiao, *J. Mater. Chem. A*, 2018, 6, 3084
62. Y. F. Ai, S.-C. Wu, K. Y. Wang, T.-Y. Yang, M. J. Liu, H.-J. Liao, J. C. Sun, J.-H. Chen, S.-Y. Tang, D. C. Wu, T.-Y. Su, Y.-C. Wang, H.-C. Chen, S. Zhang, W.-W. Liu, Y.-Z. Chen, L. Lee, J.-H. He, Z. M. Wang and Y.-L. Chueh, *ACS Nano*, 2020, 14, 8539
63. J. Liu, Z. Li, X. Huo and J. Li, *J. Power Sources*, 2019, 422, 49
64. J. Jiang, H. Li, J. X. Huang, K. Li, J. Zeng, Y. Yang, J. Q. Li, Y. H. Wang, J. Wang and J. B. Zhao, *ACS Appl. Mater. Interfaces*, 2017, 9, 28486
65. J. Wei, W. Chen, D. Chen and K. Yang, *J. Electrochem. Soc.*, 2017, 164, A2304
66. N. Zhu, F. Wu, Z. H. Wang, L. M. Ling, H. Y. Yang, Y. N. Gao, S. N. Guo, L. M. Suo, H. Li, H. J. Xu, Y. Bai and C. Wu, *J. Energy Chem.*, 2020, 51, 72
67. Z. Li, B. Niu, J. Liu, J. Li and F. Kang, *ACS Appl. Mater. Interfaces*, 2018, 10, 9451
68. S. Wang, Z. Yu, J. Tu, J. Wang, D. Tian, Y. Liu and S. Jiao, *Adv. Energy Mater.*, 2016, 6, 1600137
69. A. Lv, S. Lu, M. Wang, H. Shi, W. Yan and S. Jiao, *J. Energy Chem.*, 2022, 69, 35
70. W. Xing, D. Du, T. Cai, X. Li, J. Zhou, Y. Chai, Q. Xue and Z. Yan, *J. Power Sources*, 2018, 401, 6
71. T. Cai, L. Zhao, H. Hu, T. Li, X. Li, S. Guo, Y. Li, Q. Xue, W. Xing, Z. Yan and L. Wang, *Energy Environ. Sci.*, 2018, 11, 2341
72. W. Yang, H. Lu, Y. Cao, B. Xu, Y. Deng and W. Cai, *ACS Sustain. Chem. Eng.*, 2019, 7, 4861
73. S. Guo, H. Yang, M. Liu, X. Feng, H. Xu, Y. Bai and C. Wu, *ACS Appl. Energy Mater.*, 2021, 4, 7064
74. M. R. Lukatskaya, O. Mashtalir, C. E. Ren, Y. Dall'Agnese, P. Rozier, P. L. Taberna, M. Naguib, P. Simon, M. W. Barsoum and Y. Gogotsi, *Science*, 2013, 341, 1502
75. A. VahidMohammadi, A. Hadjikhani, S. Shahbazmohamadi and M. Beidaghi, *ACS Nano*, 2017, 11, 11135
76. M. H. Alfaruqi, S. Lee, H. Kang, B. Sambandam, V. Mathew, J.-Y. Hwang and J. Kim, *J. Phys. Chem. C*, 2022, 126, 9209
77. P. Canepa, G. S. Gautam, D. C. Hannah, R. Malik, M. Liu, K. G. Gallagher, K. A. Persson and G. Ceder, *Chem. Rev.*, 2017, 117, 4287
78. S. He, D. Zhang, X. Zhang, S. Liu, W. Chu and H. Yu, *Adv. Energy Mater.*, 2021, 11, 2100769
79. G. Cohn, L. Ma and L. A. Archer, *J. Power Sources*, 2015, 283, 416
80. T. Gao, X. G. Li, X. W. Wang, J. K. Hu, F. D. Han, X. L. Fan, L. M. Suo, A. J. Pearse, S. B. Lee, G. W. Rubloff, K. J Gaskell, M. Noked and C. S. Wang, *Angew. Chem. Int. Ed.*, 2016, 128, 10052
81. X. Yu, M. J. Boyer, G. S. Hwang and A. Manthiram, *Chem*, 2018, 4, 586
82. X. Yu and A. Manthiram, *Adv. Energy Mater.*, 2017, 7, 1700561
83. D. Zhang, X. Zhang, B. Wang, S. He, S. Liu, M. Tang and H. Yu, *J. Mater. Chem. A*, 2021, 9, 8966
84. Y. Guo, H. Jin, Z. Qi, Z. Hu, H. Ji and L. J. Wan, *Adv. Funct. Mater.*, 2019, 29, 1807676
85. Y. Guo, Z. Hu, J. Wang, Z. Peng, J. Zhu, H. Ji and L. J. Wan, *Angew. Chem. Int. Ed.*, 2020, 132, 23163
86. K. Zhang, T. H. Lee, J. H. Cha, H. W. Jang, M. Shokouhimehr and J.-W. Choi, *Electron. Mater. Lett.*, 2019, 15, 720
87. R. Fehrmann, N. Bjerrum and H. Andreasen, *Inorg. Chem.*, 1975, 14, 2259
88. R. Marassi, G. Mamantov and J. Chambers, *Inorg. Nucl. Chem. Lett.*, 1975, 11, 245
89. M. Matsunaga, M. Morimitsu and K. Hosokawa, *J. Electrochem. Soc.*, 1995, 142, 2910
90. J. Robinson and R. Osteryoung, *J. Electrochem. Soc.*, 1978, 125, 1454
91. X. Huang, Y. Liu, C. Liu, J. Zhang, O. Noonan and C. Yu, *Chem. Sci.*, 2018, 9, 5178
92. H. Lei, S. Jiao, J. Tu, W.-L. Song, X. Zhang, M. Wang, S. Li, H. Chen and D. Fang, *Chem. Eng. J.*, 2020, 385, 123452
93. Z. Li, J. Liu, X. Huo, J. Li and F. Kang, *ACS Appl. Mater. Interfaces*, 2019, 11, 45709
94. Z. Li, X. Wang, X. Li and W. Zhang, *Chem. Eng. J.*, 2020, 400, 126000
95. T. Zhang, T. Cai, W. Xing, T. Li, B. Liang, H. Hu, L. Zhao, X. Li and Z. Yan, *Energy Stor. Mater.*, 2021, 41, 667
96. T. Lu, Z. Zhang, B. Chen, S. Dong, C. Wang, A. Du, L. Wang, J. Ma and G. Cui, *Mater. Today Energy*, 2020, 17, 100450
97. H. Jiao, D. Tian, S. Li, C. Fu and S. Jiao, *ACS Appl. Energy Mater.*, 2018, 1, 4924
98. X. Zhang, S. Jiao, J. Tu, W.-L. Song, X. Xiao, S. Li, M. Wang, H. Lei, D. Tian, H. Chen and D. Fang, *Energy Environ. Sci.*, 2019, 12, 1918
99. X. Zhang, M. Wang, J. Tu and S. Jiao, *J. Energy Chem.*, 2021, 57, 378
100. T. Mori, Y. Orikasa, K. Nakanishi, C. Kezheng, M. Hattori, T. Ohta and Y. Uchimoto, *J. Power Sources*, 2016, 313, 9
101. Y. Hu, H. Huang, D. Yu, X. Wang, L. Li, H. Hu, X. Zhu, S. Peng and L. Wang, *Nano-Micro Lett.*, 2021, 13, 159
102. Y. Hu, D. Ye, B. Luo, H. Hu, X. Zhu, S. Wang, L. Li, S. Peng and L. Wang, *Adv. Mater.*, 2018, 30, 1703824
103. R. Zhuang, Z. Huang, S. Wang, J. Qiao, J.-C. Wu and J. Yang, *Chem. Eng. J.*, 2021, 409, 128235
104. S. Wang, S. Jiao, J. Wang, H.-S. Chen, D. Tian, H. Lei and D.-N. Fang, *ACS Nano*, 2017, 11, 469
105. A. Lv, S. Lu, W. Yan, W. Hu and M. Wang, *Sustain. Energy Fuels*, 2021, 5, 6328
106. G. Li, M. Kou, J. Tu, Y. Luo, M. Wang and S. Jiao, *Chem. Eng. J.*, 2021, 421, 127792
107. L. Yao, S. Ju, T. Xu and X. Yu, *ACS Nano*, 2021, 15, 13662
108. Z. Li, W. Lv, G. Wu, X. Li, X. Wang and W. Zhang, *Chem. Eng. J.*, 2022, 430, 133135
109. W. Guan, L. Wang, H. Lei, J. Tu and S. Jiao, *Nanoscale*, 2019, 11, 16437
110. Y. Du, B. Zhang, W. Zhang, H. Jin, J. Qin, J. Wan, J. Zhang and G. Chen, *Energy Stor. Mater.*, 2021, 38, 231
111. D. J. Kim, D.-J. Yoo, M. T. Otley, A. Prokofjevs, C. Pezzato, M. Owczarek, S. J. Lee, J. W. Choi and J. F. Stoddart, *Nat. Energy*, 2019, 4, 51
112. S. Wang, S. Huang, M. Yao, Y. Zhang and Z. Niu, *Angew. Chem. Int. Ed.*, 2020, 59, 11800
113. M. Walter, K. V. Kravchyk, C. Böfer, R. Widmer and M. V. Kovalenko, *Adv. Mater.*, 2018, 30, 1705644
114. X. Han, S. Li, W. L. Song, N. Chen, H. Chen, S. Huang and S. Jiao, *Adv. Energy Mater.*, 2021, 11, 2101446
115. D.-J. Yoo, M. Heeney, F. Glöcklhofer and J. W. Choi, *Nat. Commun.*, 2021, 12, 2386
116. J. Bitenc, N. Lindahl, A. Vizintin, M. E. Abdelhamid, R. Dominko and P. Johansson, *Energy Stor. Mater.*, 2020, 24, 379
117. D. Kong, T. Cai, H. Fan, H. Hu, X. Wang, Y. Cui, D. Wang, Y. Wang, H. Hu, M. Wu, Q. Xue, Z. Yan, X. Li, L. Zhao and W. Xing, *Angew. Chem. Int. Ed.*, 2022, 61, e202114681

DOI: 10.54227/mlab.20220055

Biographies

Yueqi Kong received her PhD degree (2022) from the University of Queensland (Australia). She is currently a postdoctoral research fellow under the supervision of Prof. Chengzhong Yu and Dr. Xiaodan Huang at the University of Queensland (Australia). Her research focuses on the design and synthesis of electrode materials for Rechargeable aluminium batteries.

Nashaat Ahmed received his Bachelor (2012) and Master degree (2018) at Beni Suef University (Egypt). He is currently a Ph.D. student under the supervision of Prof. Chengzhong Yu and Dr. Xiaodan Huang at the University of Queensland (Australia). His research focuses on the constructing portable rechargeable aluminium batteries by improving assembly technology, including design separators, and optimizing electrodes.

Shuimei Chen received her Master degree in China University of Geosciences, Wuhan in 2019. She is currently a Ph.D. student under the supervision of Dr. Xiaodan Huang and Prof. Chengzhong Yu at the University of Queensland (Australia). Her research focuses on the design and synthesis of electrode materials for rechargeable aluminium ion batteries.

Dmitrii Rakov received his PhD degree in Deakin University (Australia) in 2022 under the supervision of Prof. Maria Forsyth. He is currently a postdoctoral research fellow under the supervision of Prof. Chengzhong Yu and Dr. Xiaodan Huang at the University of Queensland (Australia). His research focuses on the optimization of the charge transfer mechanism in energy storage devices.

Ashok Kumar Nanjundan received his PhD degree in Materials Chemistry from Pukyong National University (Korea) in 2010 and then worked as a research fellow at Atomic Energy and Alternative Energies Commission, France, Trinity College Dublin, Kumamoto University, and the University of Queensland until 2019. He is currently the chief scientific officer of Graphene Manufacturing Group Ltd. (Australia) and holds adjunct professor positions at the University of Queensland and Queensland University of Technology. Dr. Ashok Kumar Nanjundan has over 20 years of academic and commercial chemical and materials engineering experience focused on carbon nanomaterials (graphene) for energy storage and conversion applications.

Chengzhong Yu received his PhD degree in Chemistry from Fudan University (China) in 2002 and then worked as a professor at Fudan University until 2010. He is currently a professor at the University of Queensland (Australia) and East China Normal University. His research focuses on nanoporous materials and nanostructured composites for applications in biotechnology, clean energy, and environmental protection.

Xiaodan Huang received his Bachelor (2007) and PhD degrees (2012) Chemistry from Fudan University (China). He is currently an Advance Queensland Research Fellow in Professor Chengzhong Yu's group at the University of Queensland (Australia). His research focuses on the design and synthesis of novel nanostructured materials for energy storage and environmental protection.